

Electronic transport calculations for self-assembled mono-layers of 1,4-phenylene diisocyanide on Au(111) contacts

Robert Dahlke and Ulrich Schollwöck
*Sektion Physik and Center for Nanoscience, LMU München,
Theresienstrasse 37, 80333 München, Germany*

(Dated: October 8, 2003)

We report on electronic transport calculations for self-assembled mono-layers (SAM) of 1,4-phenylene diisocyanide on Au(111) contacts. Experimentally one observes more structure (i.e peaks) within the measured conductance curve for this molecule with two cyanide end-groups, compared to measurements with molecules having thiol end-groups. The calculations are performed on the semi-empiric extended Hückel level using elastic scattering quantum chemistry (ESQC) and we investigate three possible explanations for the experimental findings. Comparing the experimental and theoretical data, we are able to rule out all but one of the scenarios. The observed additional peaks are found to be only reproduced by a mono-layer with additional molecules perturbing the periodicity. It is conjectured that the weaker coupling to Au of cyanide end-groups compared to thiol end-groups might be responsible for such perturbations.

PACS numbers: 85.65.+h, 73.23.-b, 72.10.-d

I. INTRODUCTION

Within the last decade an increasing interest in molecular electronics has developed, with the expectation of realising molecular diodes and transistors. This is based on the progress in manipulation techniques, which now allow the controlled attachment of atomic scale structures like molecules to mesoscopic leads. With these new devices one is able to determine the conductance properties of molecular structures. Explaining and predicting the electronic behaviour of such devices is an essential step towards their design and use as nano-scale electronic circuits.

To this end a number of theoretical studies have been performed with the aim of reproducing measured IV characteristics. These studies differ in the way they take the electronic levels of the molecules, their modification by the coupling to the leads and the change of electrostatic potential due to bias into account. Semi-empiric methods^{1,2,3} have been used, as well as first principles techniques,^{4,5,6,7} the latter being restricted to systems of moderate size.

The wide range of experimentally observed behaviour (see section II) suggests, that not only the structure of the molecule, but also the details of the device fabrication affect the conduction properties of molecular devices. The crucial step is the deposition of molecules onto the surface of the lead. As this is achieved by self-assembly the amount of adsorbed molecules and their individual positions can not be exactly controlled and therefore remains unknown. A satisfactory understanding of the interplay between geometrical alignment of the molecules and measured conductance properties has thus not yet been achieved (for a recent review see e.g. Nitzan et al.⁸).

In this paper we study the way in which changing the geometrical alignment of the mono-layer has an influence on the conduction properties of a molecular device. In so doing we can rule out a number of explanations which

have previously been considered⁹ to explain the occurrence of additional structure in the conductance-voltage (CV) characteristics.

The outline is the following: first we summarise some of the recent experimental findings. Then the method we use (based on ESQC¹⁰) for calculating the conductance properties of molecular devices, is discussed. Calculations for the conductance of a SAM, being build of 1,4-phenylene diisocyanide (PDI) and sandwiched between gold leads are then presented. The results for three qualitatively different geometrical constitutions of the mono-layer are compared with experimental data. By this we can rule out all but one and conclude that the only geometrical alignment, which gives rise to several peaks in the conductance curve, is a mono-layer with additional molecules perturbing the periodicity.

II. EXPERIMENTAL OVERVIEW

The devices built to study conductance properties of molecular structures differ not only in amount and chemical structure of the molecules in use but also in the way these are attached to metallic or semi-conducting leads. Single or few molecules are accessible in mechanically controllable break junctions (MCB) and with the scanning tunneling microscope (STM). Many molecules are involved in sandwiched self-assembled mono-layer (SAM) experiments. The observed properties depend on the exact geometry of the device. The conductance differs in orders of magnitude and the qualitative voltage dependency of the current ranges from simple ohmic behaviour to negative differential resistance (NDR).¹¹

In the past Reed et al.¹² have measured the electrical conductance of a self-assembled molecular mono-layer bridging an MCB at room temperature. Molecules of 1,4-benzene dithiol (i.e. having two thiol end-groups, which are known to couple strongly to Au-atoms) were used

and the CV characteristic was found to be symmetric with one peak in the voltage range of $0 - 2V$. They measured a current of the order of $50nA$ at a bias voltage of $2V$, which they claim is produced by transport through one single active molecule. Reichert et al.¹³ also used an MCB with molecules having two thiol end groups, but being considerably longer. The measured current amplitude was about $500nA$ at $1V$, i.e. although the molecule was more than twice as long, the current was ten times larger.

With a different setup, where a SAM is sandwiched between two metallic leads, Chen et al.¹¹ have found negative differential resistance (NDR), namely one peak at $2V$ in the IV curve. The molecule under investigation had one thiol end-group only and was attached to Au-leads at both ends. The measurements were taken at room temperature and the measured current maximum was of the order of $1nA$.

Only recently, sandwiched SAM devices at $4.2K$ were studied,^{9,14} where a benzene ring with two cyanide instead of thiol end-groups was used. The measurements exhibited currents of the order of $50 - 400nA$. The CV characteristic for this molecule revealed more structure, in form of three to five peaks within a voltage range of $1V$. Such a behaviour was not observed with previous devices containing other molecules.

III. THEORETICAL FORMALISM

In the literature there has been presented quite a number of techniques to calculate non-equilibrium electronic transport through molecular systems attached to mesoscopic leads. Usually the Landauer formalism is applied, which describes current as elastic electron transmission and therefore requires the transmission function $T(E)$. To this end one needs a framework that allows for a description of the molecular device on the atomic level. This involves not only the molecules themselves, but also the surface and bulk region of the leads. Quantum chemistry provides such a framework, and one can choose the level of theory according to the size of the system under consideration and the computational effort one is willing to spend.

Using a quantum chemistry method, the transmission function can be obtained from an effective one-particle Hamiltonian, which is an appropriate description for strong coupling of the molecules to the leads (as in the case of covalent binding). The methods differ in the generation of the one-particle Hamiltonian, which might be based on semi-empirical grounds^{1,2,3} or on first-principles and self-consistent techniques.^{4,5,6,7}

A different approach,¹⁵ taking many-particle effects explicitly into account, uses a master equation with transition rates calculated perturbatively using the golden rule. This approach is appropriate for weak coupling.

We use the Landauer formalism, as the molecules are assumed to be chemically bonded to the gold contacts

(i.e. strong coupling), together with the semi-empiric extended Hückel quantum-chemistry method ESQC.¹⁰ The molecular structure is optimised¹⁶ beforehand. This approach, though limited as compared to more sophisticated quantum chemistry methods, is yet justified, because we want to gain a qualitative understanding of a many molecule experiment, which can not be described by first-principle techniques, as the number of atoms involved is beyond the practical limitations of to-date computer resources.

A. Landauer formalism

According to the Landauer formula, current along a defect region is the result of electron transmission from the source to the drain lead. This is described by the transmission function $T(E)$ and net electron transfer happens at all those energies, where there are more states occupied in the source lead than in the drain. The difference in occupation is a result of the applied bias V , which raises the chemical potential μ_1 of the source lead above the one of the drain lead $\mu_2 = \mu_1 - eV$ and thus changes the distribution function $f_i(E) = f(E - \mu_i)$.

$$I = \frac{-2e}{h} \int_{-\infty}^{\infty} T(E) (f(E - \mu_1) - f(E - \mu_2)) dE. \quad (1)$$

The Landauer formula is valid under the condition that transport is coherent across the molecule, which is plausible as the typical mean-free path of electrons within metals is of the order of $500nm$, while the molecular gap between source and drain lead is only about $1 - 5nm$ in length. Furthermore it is assumed that the coupling of the leads to macroscopic reservoirs is reflection-less, and that the tunneling electrons equilibrate only deep inside the leads. This ensures that the distribution function for incoming electrons in a lead can be taken to be spatially constant, even close to the molecular region.

The system is formally partitioned into three regions $\Sigma_i, i \in \{0, 1, 2\}$, two of them ($\Sigma_{1,2}$) containing the semi-infinite leads, the third one (Σ_0) being the finite region containing all molecules as well as a few surface layers of each lead (see Fig. 1). We use periodic boundary conditions in the directions perpendicular to the surface normal.

By a tight binding approximation, the infinite-dimensional Hamiltonian of the entire system can be composed of quantum chemical one-particle block Hamil-

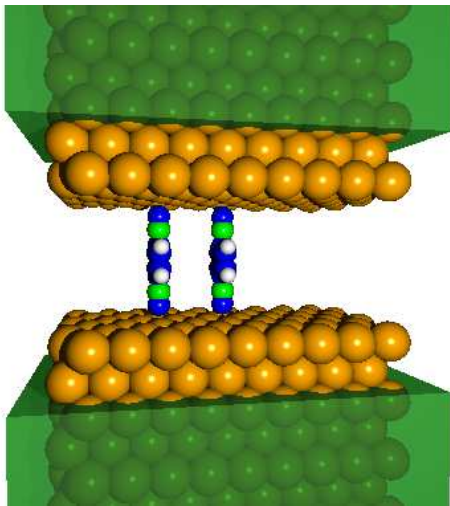


FIG. 1: (Colour online) Partitioning of the system into three parts: the two semi-infinite leads $\Sigma_{1,2}$ (surrounded by boxes) and the molecular region Σ_0 between them.

tonians of finite dimension:

$$\begin{aligned}
H = & \sum_{i \in \text{mol}} (\varepsilon_i c_{mi}^\dagger c_{mi} + \sum_{j \neq i} H_{ij}^m c_{mi}^\dagger c_{mj}) \\
& + \sum_{d \in \text{leads}} \sum_{l=l_0}^{\infty} \sum_{i \in l} (\varepsilon_{di} c_{di}^\dagger c_{di} + \sum_{j \neq i} H_{lij}^d c_{di}^\dagger c_{dlj}) \\
& + \sum_{d \in \text{leads}} \sum_{l=l_0}^{\infty} \sum_{\substack{i \in l \\ j \in l+1}} (H_{l,l+1,i,j}^d c_{di}^\dagger c_{d,l+1,j} + \text{h.c.}) \\
& + \sum_{d \in \text{leads}} \sum_{i \in l_0} \sum_{j \in \text{mol}} (H_{l_0 i j}^{dm} c_{d l_0 i}^\dagger c_{mj} + \text{h.c.}) \quad (2)
\end{aligned}$$

The first summation describes the isolated molecular region, by an on-site energy ε and a hopping term. The indices i and j run over the orbital basis set within that region. The next two summations describe the isolated leads, labelled by d . Layer by layer, starting with the surface layer l_0 , the first term accounts for intra-layer interactions, while the second one describes the interaction between layers. (The size of each layer is chosen such that only adjacent layers have non-zero interaction. It therefore depends on the details of the tight-binding approximation.) Finally the last term describes the coupling between the molecular region and each lead. Note that only the first layer l_0 contributes to that term and that there is no interaction between different leads. These are only formal restrictions, as parts of each lead can be included into the molecular region.

The determination of the transmission function involves two steps. First the conduction properties of the isolated leads have to be calculated. Thereby each lead will be decomposed into conducting and non-conducting in- and out-going channels. These correspond to propagating and evanescent solutions moving in one of two possible directions respectively. In a second step, the

channels are connected to each other via the molecular region. This is described by the scattering matrix and the transmission function is finally obtained by summing up the contribution from each channel.

The calculation can be performed either using Green's function techniques¹⁷ or equivalently¹⁸ using ESQC^{10,19}, which is a scattering-matrix approach. We present the details of the calculation in the second scheme, as individual contributions from each channel to the transmission function can then be easily studied.

B. Bulk propagator

First we will restrict our attention to the semi-infinite lead Hamiltonians, which do not have to be identical. The Hamiltonians of equation (2) for one lead $H_{ll'}^d$ are layer independent, if one assumes periodicity, i.e. $H_{ll'}^d = H_{l_0 l_0}^d$ and $H_{l,l+1}^d = H_{l_0, l_0+1}^d$. Using Bloch's theorem one can reduce the infinite dimensional system of equations to an $N \times N$ -matrix equation (N being the number of orbital basis functions in one layer)

$$(M(E) + h(E)e^{ik\Delta} + h^\dagger(E)e^{-ik\Delta}) \gamma(k, E) = 0, \quad (3)$$

with $M(E) := H_{l_0 l_0} - E S_{l_0 l_0}$, $h(E) := H_{l_0, l_0+1} - E S_{l_0, l_0+1}$, and $S_{ll'}$ is the overlap matrix between orbitals in layer l and layer l' for cases when one does not deal with an orthonormal basis set (otherwise $S_{ll'} = \text{Id} \cdot \delta_{ll'}$). With Δ we denote the lattice spacing. Defining $\lambda := e^{ik\Delta}$ one can easily see that equation (3) is an $N \times N$ quadratic eigenvalue equation. It can be transformed into a $2N \times 2N$ linear eigenvalue equation:

$$P(E) \begin{pmatrix} \gamma_1 \\ \gamma_2 \end{pmatrix} = \lambda(E) \begin{pmatrix} \gamma_1 \\ \gamma_2 \end{pmatrix}, \quad (4)$$

$$P := \begin{bmatrix} 0 & 1 \\ -h^{-1}h^\dagger & -h^{-1}M \end{bmatrix} \quad (5)$$

(where we have dropped the energy dependency for notational ease). This layer-to-layer propagator P reduces the problem of finding solutions for the entire isolated lead Hamiltonian to specifying the wave function coefficients at two adjacent layers γ_l and γ_{l+1} only. This is due to the fact that given these coefficients any other pair of coefficients γ_{l+2k} , γ_{l+2k+1} can now be obtained via:

$$\begin{pmatrix} \gamma_{l+2k} \\ \gamma_{l+2k+1} \end{pmatrix} = P^k \begin{pmatrix} \gamma_l \\ \gamma_{l+1} \end{pmatrix}. \quad (6)$$

All possible solutions at energy E can be decomposed into independent channels, by solving for the eigenvalues of equation (4). These eigenvalues come in pairs such that for each eigenvalue $\lambda_>$, there exists a corresponding eigenvalue $\lambda_<$ satisfying the relation $\lambda_> = 1/\lambda_<^*$, as can be seen by transposing equation (3). Eigenvalues with $|\lambda| \neq 1$, i.e. complex k , belong to exponentially diverging solutions (see equation (6)). These are of course non physical, as long as the lead is infinite. In semi-infinite

leads however (which we are dealing with), exponentially decaying coefficients at the boundary will contribute to the surface wave function and must not be neglected.

C. Current operator

The contribution from a single channel to the net current can not directly be seen from equation (4). It depends on the current density associated with a solution to the Schrödinger equation $i\hbar\partial_t S\gamma = H\gamma$ and is obtained via the continuity equation. The probability amplitude $|\gamma|^2$ for a stationary solution is constant in time

$$\frac{\partial}{\partial t}\gamma^\dagger S\gamma = \frac{i}{\hbar}(\gamma^\dagger H\gamma - \gamma^\dagger H^\dagger\gamma) = 0, \quad (7)$$

because H and S are hermitian. For the probability amplitude at all layers between l_1 and l_2 one therefore has

$$\begin{aligned} 0 &= \frac{\partial}{\partial t} \sum_{l=l_1}^{l_2} (\gamma_l^\dagger \gamma_l) \\ &= \frac{i}{\hbar} \sum_{l=l_1}^{l_2} \gamma_l^\dagger (H - H) \gamma_l \\ &= \frac{i}{\hbar} (\gamma_{l_1-1}^\dagger h(E) \gamma_{l_1} + \gamma_{l_1+1}^\dagger h^\dagger(E) \gamma_{l_1} - \text{h.c.}) \\ &\quad + \frac{i}{\hbar} (\gamma_{l_2-1}^\dagger h(E) \gamma_{l_2} + \gamma_{l_2+1}^\dagger h^\dagger(E) \gamma_{l_2} - \text{h.c.}) \\ &= \langle \gamma | l_2, l_2 + 1 \rangle \frac{i}{\hbar} \begin{bmatrix} 0 & -h \\ h^\dagger & 0 \end{bmatrix} \langle l_2, l_2 + 1 | \gamma \rangle \\ &\quad - \langle \gamma | l_1 - 1, l_1 \rangle \frac{i}{\hbar} \begin{bmatrix} 0 & -h \\ h^\dagger & 0 \end{bmatrix} \langle l_1 - 1, l_1 | \gamma \rangle, \end{aligned} \quad (8)$$

with the projectors $\langle l | \gamma \rangle := \gamma_l$. This gives rise to the definition of the current operator W_l for layer l as

$$W_l := |l, l + 1\rangle \frac{i}{\hbar} \begin{bmatrix} 0 & -h \\ h^\dagger & 0 \end{bmatrix} \langle l, l + 1|. \quad (9)$$

Now let both φ and ϑ be solutions at fixed energy E with the eigenvalues λ_1 and λ_2 respectively. Because the expectation value for W_l is layer independent (equation 8) one has:

$$\begin{aligned} \langle \vartheta | W_l | \varphi \rangle &= \langle \vartheta | W_{l+1} | \varphi \rangle \\ &= \lambda_1^* \lambda_2 \langle \vartheta | W_l | \varphi \rangle. \end{aligned} \quad (10)$$

This equation describes the connection between the current properties of a solution φ and its eigenvalue λ . We summarise the results of a detailed analysis of this equation, which is given in appendix A. Each channel $|\varphi_i\rangle$ can be assigned a current value v_i , defined as

$$v_i := \text{Im} \langle \varphi_i | W | \varphi_i \rangle, \quad (11)$$

where we have used the layer independence of W_l in simply writing W .

Channels with eigenvalue modulus $|\lambda| \neq 1$, i.e. evanescent waves have zero current value. They therefore do not contribute to the current. (Yet they are important at the surface, as already mentioned above.)

Only channels with an eigenvalue of modulus one ($|\lambda| = 1$) contribute to the current. The sign of v_i determines the direction of charge transport.

Therefore the eigenvalues can be sorted into incoming and outgoing solutions ($\lambda_>$ and $\lambda_<$ respectively), according to the following scheme: if $|\lambda| < 1$ it represents an incoming evanescent solution, if $|\lambda| > 1$ then it is outgoing evanescent. Only if $|\lambda| = 1$ it belongs to a propagating solution, which is incoming for $v > 0$ and outgoing otherwise.

We now define $\Lambda_>$ and $\Lambda_<$ as the two $N \times N$ diagonal matrices composed of all incoming and outgoing eigenvalues $\Lambda_{\gtrless} := \text{diag}(\lambda_{\gtrless}^i)$. The $2N \times 2N$ -matrix U , which diagonalises P :

$$U^{-1} P U = \begin{bmatrix} \Lambda_> & 0 \\ 0 & \Lambda_< \end{bmatrix}, \quad (12)$$

has the following quadratic block form:

$$\begin{bmatrix} U_> & U_< \\ U_>\Lambda_> & U_<\Lambda_< \end{bmatrix}. \quad (13)$$

After this transformation into the diagonal basis of the propagator, we can easily obtain all physically relevant solutions of the infinite lead by specifying the amplitudes of all propagating waves at one lattice site.

D. Scattering matrix

Up to now, we have considered the isolated leads only. These are now assumed to be each coupled to the molecular defect region and thereby indirectly coupled to one another. We are interested in stationary solutions, which consist of an incoming propagating wave in one lead, being scattered among all the accessible outgoing channels (propagating and evanescent ones). This information is contained in the scattering matrix S

$$\begin{pmatrix} \mathcal{B} \\ \mathcal{C} \end{pmatrix} = \underbrace{\begin{bmatrix} s_{11} & s_{12} \\ s_{21} & s_{22} \end{bmatrix}}_{=:S} \begin{pmatrix} \mathcal{A} \\ \mathcal{D} \end{pmatrix}, \quad (14)$$

which determines the wave amplitudes of all outgoing waves \mathcal{B}, \mathcal{C} given the incoming ones \mathcal{A}, \mathcal{D} . In appendix B it is shown, that S is of the form

$$S = -M_{\text{in}}^{-1} \cdot M_{\text{out}}. \quad (15)$$

It is important to notice, that the scattering matrix is always quadratic, because in each lead there are the same amount of incoming and outgoing channels. This is opposed to the transfer matrix T_{transf} , which determines

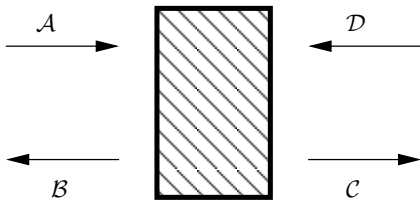


FIG. 2: Incoming and outgoing wave amplitudes.

the amplitudes of in- and outgoing waves C, D in one lead given the in- and outgoing waves A, B of a second lead:

$$\begin{pmatrix} C \\ D \end{pmatrix} = T_{\text{transf}} \begin{pmatrix} A \\ B \end{pmatrix}. \quad (16)$$

This matrix is quadratic only if both leads have the same number of channels. It then is of the form²⁰

$$T_{\text{transf}} = \begin{bmatrix} F & G^\dagger \\ G & F^\dagger \end{bmatrix} \quad (17)$$

and the relation to the scattering matrix is²⁰

$$S = \begin{bmatrix} -F^\dagger(-1)G & F^\dagger(-1) \\ F^{-1} & G^\dagger F^\dagger(-1) \end{bmatrix}. \quad (18)$$

Methods calculating the scattering matrix via the transfer matrix¹⁹ fail, if two types of leads are used, because F is then no longer quadratic and can not be inverted. Therefore one commonly takes source and drain lead to be identically constituted. But even in such cases, the method becomes numerically unstable, with increasing distance between the molecular region and one lead. This is because the matrix elements of F and G (in equation (17)) diverge exponentially, with increasing lead separation. Taking the inverse of F is therefore a numerically critical procedure. Both these problems are avoided by the direct calculation of the scattering matrix, which we present in appendix B. This calculation is well defined without any restrictions to the number of leads and their composition. That means that it is not necessary to restrict to identical leads. Furthermore it allows a numerically stable determination of the scattering matrix, even for weak coupling.

E. Transmission function

The transmission function is the sum over the contributions from each combination of incoming channel in the source lead to outgoing channel in the drain lead: $T(E) = \sum_{i,j} T_{j \leftarrow i}$. The relation between scattering matrix S and these transmission function elements is

$$T_{j \leftarrow i} = |(s_{21})_{j \leftarrow i}|^2 \frac{v_j}{v_i}, \quad (19)$$

where s_{21} is the lower left block of S as defined in equation (14). The weighting with velocity factors comes

about because the scattering matrix s does not relate current densities, but wave amplitudes. The current densities are obtained from these wave amplitudes by multiplication with the corresponding velocity factor v_j . The factor v_i in the denominator normalises the transmission function to be exactly one for perfect transmission. If $v_i = 0$ then $T_{j \leftarrow i} = 0$, because incoming evanescent waves have zero amplitude at the surface.

The total current is made up of the contribution from each k -state¹⁷:

$$\begin{aligned} I &= -\frac{e}{V} \sum_{k,\sigma} \sum_{i,j} v_i T_{j \leftarrow i}(E_k) \underbrace{(f(E_k - \mu_1) - f(E_k - \mu_2))}_{=:\Delta f(E_k)} \\ &= -\frac{e}{V} \sum_{k,\sigma} \sum_{i,j} \frac{\partial E_k}{\hbar \partial k} T_{j \leftarrow i}(E_k) \Delta f(E_k) \\ &= -\frac{2e}{h} \int_{-\infty}^{\infty} dE \sum_{i,j} T_{j \leftarrow i}(E) \Delta f(E) \\ &= -\frac{2e}{h} \int_{-\infty}^{\infty} T(E) \Delta f(E) dE. \end{aligned}$$

Here the summation over k has been transformed into an integral over E with a factor of 2 accounting for spin σ .

IV. CALCULATIONS FOR PDI

Low temperature experiments with PDI SAM's sandwiched between two metallic leads show several peaks in the CV -diagram.^{9,14} The typical voltage differences of these peaks are in the range of $\Delta U \approx 0.2V$ (i.e. there are about 5 peaks within $U = 0V$ and $U = 1V$). The commonly adopted explanation for the occurrence of such peaks is the following. Each molecular orbital that enters the energy window, which is opened by the applied voltage, enables resonant tunneling. This increases the conductance and therefore results in a peak within the CV -diagram.

Typically, the energy gap between molecular orbitals is in the range of $\Delta E \approx 1eV$. In other words, for applied voltages up to $U = 1V$ there should be only a single accessible orbital per molecule, giving rise to only a single peak in the CV -diagram. Therefore the following question arises: are there geometrical alignments of the molecules such that the additional peaks in the CV diagram can also be explained by resonant tunneling through molecular orbitals?

A. Influence of changes in the molecular alignment to the transmission spectrum

During the device fabrication, the step under least experimental control is the adsorption of the molecules onto the leads. Therefore the exact geometrical alignment of the molecular SAM and, at least in the sandwich geometry, also the atomic shape of the top metallic lead, is

not exactly known. One therefore has to expect not only one specific but rather quite a variety of molecular alignments to be produced. As one is interested in the conduction properties of the resulting device, it is important to understand the influence of each type of geometrical alignment to the transmission function.

To this end, we have investigated three such possible alignments, which will be discussed separately.

1. By adding metal-atoms on top of the molecular mono-layer in a random way, there might occur metallic clusters on top of the mono-layer. These affect the electronic configuration of the molecules individually, and might therefore have an influence to the transmission function.
2. In a SAM experiment, there is not just one molecule, but rather a few hundred molecules involved. If the contribution to the transmission function was different for each molecule, then $T(E)$ would change qualitatively, with a change in size of the mono-layer. We therefore analyse how the transmission functions depends on the number of molecules involved.
3. If the molecular mono-layer is not strictly periodic, then there will be defects. For example can the distance between two molecules be reduced, such that inter-molecular bonds can be build. Each of these defects will have a specific electronic structure and will therefore influence the transmission function.

1. Influence of metallic clusters

In the sandwich geometry, first the bottom metallic lead is created. Then the molecular mono-layer is adsorbed on top of it by self-assembly. Finally the top metallic lead is build upon the molecular mono-layer. The exact shape of neither metallic surface is known and may be anything but flat and regular.

It is likely that the surface atoms of the top metallic lead build up clusters on top of the molecular layer (as for example in Fig. 3 b). Which influence do they have on the electronic configuration of the molecule they are in contact with? And do the clusters act as small molecules with new electronic levels?

The influence of an Au cluster on the molecular electronic structure is twofold. First it introduces new electronic levels, and second the existing molecular electronic levels will be shifted, by an amount which depends on the strength of the coupling between cluster and molecule.

The latter effect will be observed as a shifted peak in the transmission function, only if the coupling between cluster and molecule is different to the coupling between top electrode and molecule. For clusters similar to the one shown in Fig. 3 (b), this is however not the case. The energetic peak positions are identical, as can be seen in Fig. 3 (c).

Furthermore, there are no additional peaks, which one might have expected because of the additional electronic levels of the cluster. The explanation of their absence is the following: an electronic level gives rise to a peak in the transmission function only, if the corresponding orbital wave function overlaps with both the top and bottom electrode. The overlap with the electrode the cluster is attached to (say top electrode) is of course large. The overlap with the bottom electrode consists of two parts. The direct overlap and the indirect overlap via the molecule. The direct overlap is negligible due to the large spatial separation. The indirect overlap depends on the molecular orbital wave function. If the energy of the cluster level does not coincide with a molecular energy level, then there is no indirect overlap. Only if two levels coincide, the indirect coupling is large, but in that case, there already exists a transmission peak due to the molecule itself.

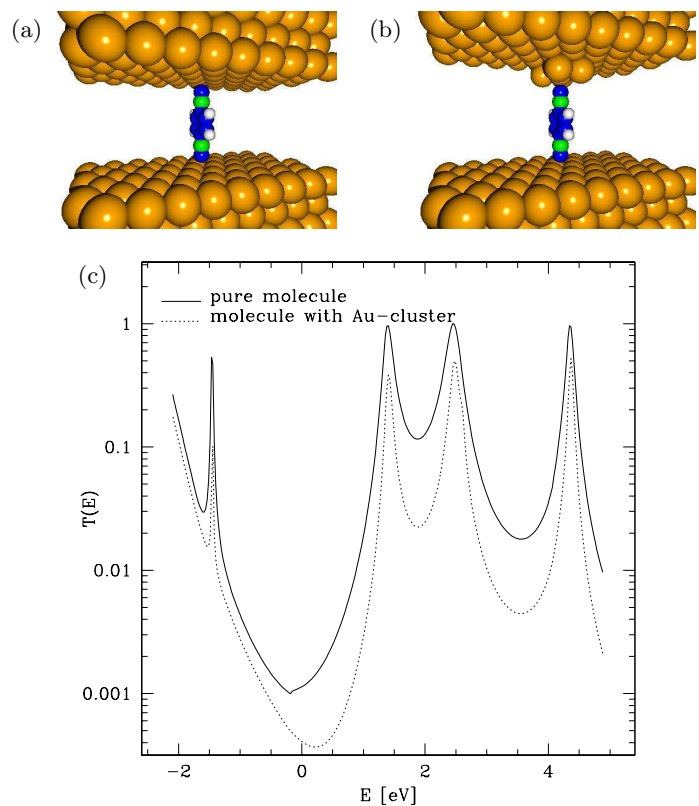


FIG. 3: (a) (Colour online) Structure for a molecule without cluster. (b) (Colour online) Structure for a molecule with a gold cluster on top. (c) Transmission function $T(E)$ for both structures. Energy scale is relative to the HOMO-LUMO gap, such that $E = 0$ corresponds to the middle of the gap.

Therefore if transmission is already suppressed by the molecule (at all off-resonant energies), it can either be further reduced by off-resonant tunneling through the cluster, or it can (at best) be left unchanged by resonant tunneling through the cluster. Under no circumstances can transmission, once suppressed by the molecule, be afterwards increased by the cluster. This in turn means,

that metallic clusters can not give rise to additional peaks in the transmission spectrum.

2. Mono-layer versus single molecule

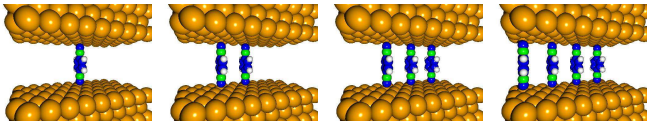


FIG. 4: (Colour online) The structure for one, two, three, and four molecules adsorbed within an Au- 9×3 super-cell. This setup was used to test the sum rule.

How do we expect the transmission function $T^i(E)$ for i periodically arranged molecules to look like? As long as the inter-molecular interactions are small (compared to the intra-molecular ones) the molecular levels of each molecule will not be significantly changed. Furthermore as the mono-layer consists of only one kind of molecule, all of them will have the same electronic structure. Therefore we expect each molecule to contribute the same amount to the transmission function: $T^n(E) := \sum_i T^1(E) = nT^1(E)$, where i runs over all n adsorbed molecules.

We calculated the transmission function for $n=1$ to 4 molecules within an Au super-cell of size 9×3 (the structures are shown in Fig. 4). The distance between the molecules is chosen to be a multiple of the closest Au-Au separation a ($d = 5.76\text{\AA} = 2a$, with $a = 2.88\text{\AA}$). To our knowledge, the parameters of the PDI-SAM mono-layer have never been determined experimentally, which is why we have to assume the above values. However STM studies²¹ and also theoretical calculations²² have been performed for alkanethiol mono-layers, and these parameters motivated our choice.

Independent from the number of molecules present, the transmission functions have the same amount of peaks, at identical energetic positions (see Fig. 5 a). This result is also obtained for all larger distances of the molecules, where the inter-molecular interaction is even smaller. Furthermore, the sum rule is indeed fulfilled, as shown in Fig. 5 (b). Each $T^i(E)$ is plotted against $T^4(E)$ for $i \in \{1, 2, 3\}$. The calculated transmission values (300 discrete values each) clearly show a linear correlation. The straight lines are linear fits to the data, and their slope does very well agree with the theoretically expected value of $a(n, m) = n/m$. The deviation is below 6%, as can be seen in table I, where we summarise all the fitted values for $T^n(E) = a(n, m) \cdot T^m(E)$.

We conclude the following: a mono-layer, where the inter-molecular distance is large enough to not let inter-molecular interactions play a significant role, has the same number of distinct electronic levels as a single molecule. These levels are then highly degenerate. A CV-diagram will therefore have the same number of

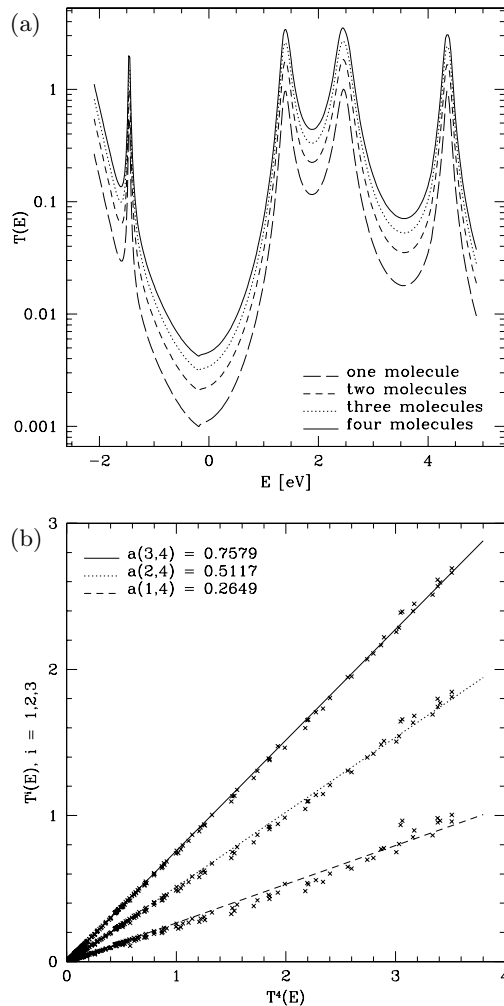


FIG. 5: (a) Transmission function for one, two, three, and four PDI molecules. (b) When plotted against each other, the transmission functions reveal a linear relationship: $T^i(E) = a(i, 4)T^4(E)$ (bottom).

peaks. Only the net current will be increased by a factor $a(n, m)$ compared to the single molecule case.

The mere fact, that one deals with a mono-layer instead of a single molecule does not imply that the transmission function changes qualitatively.

3. Influence of molecular clusters

We have seen, that one does not observe additional peaks in the transmission function, as long as the inter-molecular influence is small. And this is the case for distances which occur in typical SAM structures.^{21,22} We now investigate cases, where the molecular interactions are not negligible. This occurs for example, when the periodic structure of the mono-layer is perturbed by an additional molecule, such that a molecular cluster is formed. It is sufficient to study the transmission function of an

n	m	$a(n, m)$	$\frac{a}{n/m} - 1$	σ
1	2	0.5188	3.76%	0.014
1	3	0.3500	4.99%	0.018
1	4	0.2649	5.96%	0.021
2	3	0.6753	1.30%	0.008
2	4	0.5117	2.34%	0.015
3	4	0.7579	1.06%	0.011

TABLE I: The fitted values for $a(n, m)$ together with their deviation from the theoretical value $a(n, m) := n/m$ and a measure for the quality of the fit σ , where $\sigma^2 := (N - 1)^{-1} \sum (T^n(E_i) - a(n, m)T^m(E_i))^2$ for $N = 300$ discrete energy values $T(E_i)$.

isolated cluster only, because we have already seen that molecules in the periodic SAM arrangement do not influence each other. The sum of the transmission function for the periodic SAM and the transmission function for the molecular cluster is, due to the sum rule, the total transmission function for defect and SAM.

We study the influence of a shorter distance between two, three, and four molecules on the transmission spectrum and relate it to the discrete energies of the isolated molecules. The molecules are now separated by $d = 2.88\text{\AA}$ which corresponds to the Au-Au atom spacing. The atomic structure for this calculation is shown in Fig. 6 (a), the resulting transmission functions in Fig. 6 (b) and (c).

By reducing the molecular separation from $d_1 = 2 \cdot 2.88\text{\AA} = 5.76\text{\AA}$ to $d_2 = 2.88\text{\AA}$, the transmission function qualitatively changes. The number of peaks roughly doubles. The new peak positions are different from the ones we have obtained in the previous calculations. And this time, the peak positions do depend on the number of molecules involved. This is an important point, because if there are several molecular clusters with different molecular distances, then they all give rise to peaks at different energy values. The resulting transmission function is the sum of the individual functions and will thus contain far more peaks, than the transmission function for the non-perturbed periodic layer.

We now show that the new peaks are a result of the increase in molecular interaction due to the decrease in spatial separation. For non-interacting molecules, the molecular energies are identical and therefore degenerate. An interaction between molecules breaks this degeneracy and therefore new energy levels occur. By performing a diagonalisation of the molecular Hamiltonian (without leads) one can determine the levels of the molecular cluster.

In Fig. 7 we have again plotted the transmission function for three and four molecules, this time together with the discrete energy levels of the corresponding molecular cluster. The inset is identical to Fig. 6 (c), while the plot itself is a magnification, to better resolve the discrete energy levels (which are shown as points along the

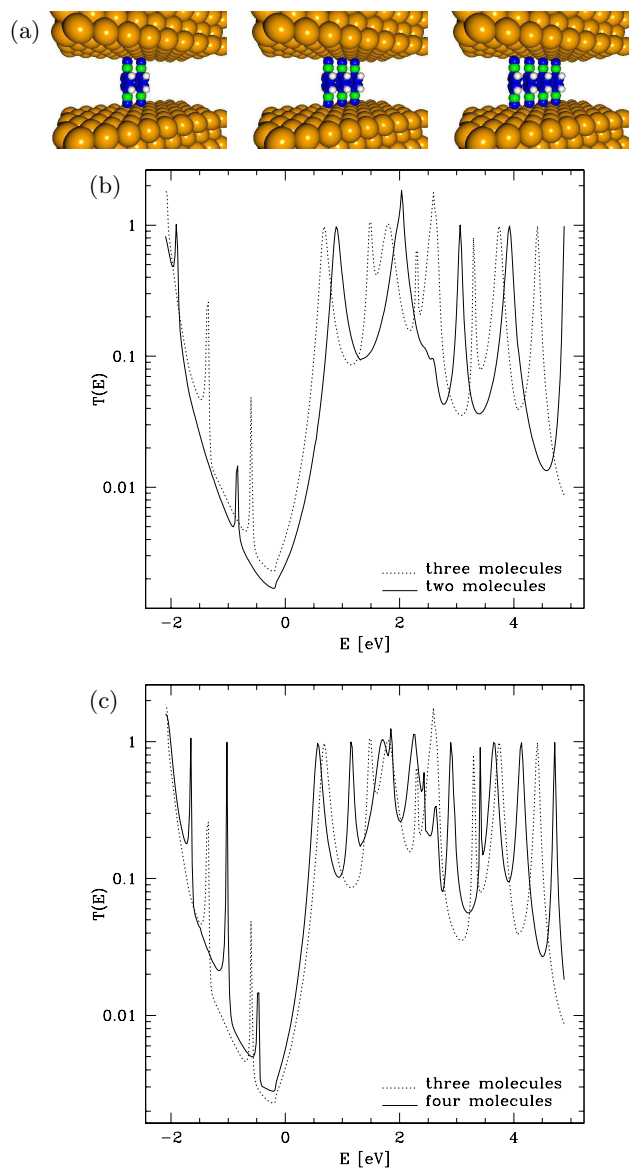


FIG. 6: (a) (Colour online) Two, three, and four molecules with a shorter inter-molecular distance. (b) The transmission functions for two and three molecules. (c) The transmission functions for three and four molecules. In contrast to all previous cases, the peaks are shifted with respect to each other and there are also additional peaks. These changes are due to the increase in inter-molecular interaction, which alters the electronic levels.

transmission function). Each of the transmission peaks is related to at least one discrete energy value. But not each energy value can be related to a peak in the transmission function. Why is that? The discrete energies can only give rise to new peaks in the transmission function, if they are not suppressed by a weak coupling to one of the leads. All levels which are not related to any peak belong to this category. If the position of the peak is shifted away from a corresponding energy level, then this is due to the coupling between molecules and leads. This

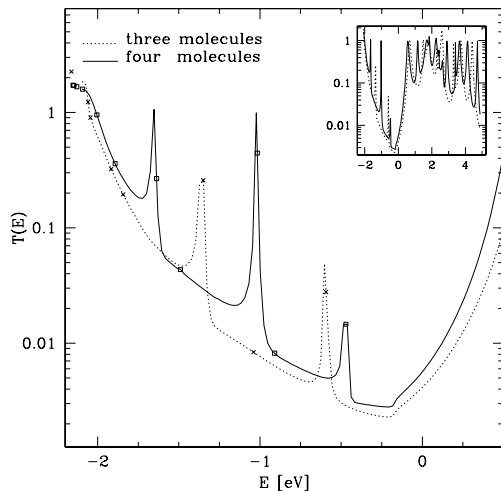


FIG. 7: Magnification of the transmission functions for three and four closely spaced molecules. Additionally the discrete energy levels of the system without leads are plotted as points along the transmission function. To each peak there belongs at least one discrete energy level. A detailed discussion is given in the main text. Inset: Transmission function (original scale) for three and four closely spaced molecules (identical to Fig. 6 c).

coupling is absent in the diagonalisation of the molecular Hamiltonian, but present in the calculation of the transmission function.

Finally we show, that the additional peak structure in the transmission function for a scenario with an increased inter-molecular interaction gives rise to a number of steps in the IV -curve. Figure 8 contains an IV calculation for a molecular structure containing all three molecular clusters shown in Fig. 6 (a). In this calculation, the bias voltage V_b enters as a shift of the Fermi levels for source and drain lead: $\mu_1 = \mu_2 + eV_b$. The molecular energy has been set to $E_m = \mu_1 - \delta E_m - \eta eV$, where δE_m is the zero bias displacement of the molecular levels and $\eta = 0.5$, because of the symmetric coupling to the leads.

Compared to the experiments^{9,14} the number of steps in the IV -curve is well reproduced by our calculation. The obtained current is at least one order of magnitude larger than the experimental values.¹⁴ This is a phenomenon common to all theoretical methods based on the Landauer formula.^{3,23} A satisfactory explanation for this discrepancy as well as for the broad range of experimentally observed current values has not yet been found.

V. DISCUSSION

We have shown, that the peak structure of the transmission function is robust against changes in the number of adsorbed molecules, as long as the distance between molecules is considerably large ($d \gtrsim 6\text{\AA}$). And also does the exact shape of the top metallic lead not influence

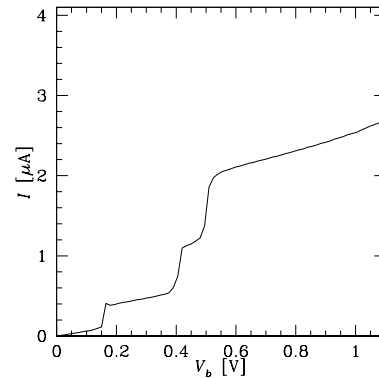


FIG. 8: IV -calculation for a molecular region containing all three molecular clusters shown in Fig. 6 (a). There are three distinct steps within the voltage range of 1V.

the qualitative structure of the transmission function. Only if the distance between molecules becomes so small, that inter-molecular interactions are no longer negligible (which is below 6\AA in our case), does the transmission function undergo a qualitative change. Namely an additional peak structure occurs.

How does this finding compare to the experimental data? As we have pointed out in section II, only in devices using molecules with two cyanide end-groups a more or less random peak structure was observed in the CV characteristic^{9,14}. In other devices, molecules with at least one thiol end-group are typically used. These show significantly less peak structure.

We therefore give the following interpretation: The thiol end-group is known to bind strongly to Au atoms. It is therefore likely, that thiol-based mono-layers stably adsorb to gold leads. Resulting periodic structures are then robust against distortions. The conductance of such structures is proportional to the corresponding single molecule conductance, i.e. the number of molecules involved changes the absolute value of the current only, not the peak structure.

The random like peak structure in devices, made up of cyanide based molecules suggests, that there are some molecular clusters present in the mono-layer. These clusters might occur, because the binding of a cyanide end-group to Au is considerably weaker compared to that of a thiol end-group, and weaker binding results in a less robust periodic structure.

Acknowledgements

We would like to thank Xavier Bouju, as well as Udo Beierlein for helpful discussions.

APPENDIX A: CONNECTION BETWEEN EIGEN- AND CURRENT-VALUES

The current properties of each channel can be related to the corresponding eigenvalue. We start from equation (10):

$$\begin{aligned}\langle\psi|W_j|\phi\rangle &= \langle\psi|W_{j+1}|\phi\rangle \\ &= \lambda_1^* \lambda_2 \langle\psi|W_j|\phi\rangle.\end{aligned}$$

Let's first consider $|\psi\rangle = |\phi\rangle$, i.e. $\lambda_1 = \lambda_2$, i.e. $\langle\psi|W_j|\phi\rangle = |\lambda|\langle\psi|W_j|\phi\rangle$. For each channel with eigenvalue $|\lambda| \neq 1$ one then must have $\langle\psi|W_j|\psi\rangle = 0$, i.e. this channel does not itself carry any current. This is consistent with our terminology of an evanescent wave. If, however, $|\lambda_i| = 1$, then $\langle\psi|W_j|\psi\rangle$ is purely imaginary, because W_j is an anti-hermitian operator. We can therefore define the velocity of a propagating wave to be $v_i := \text{Im}\langle\psi|W_j|\psi\rangle$.

Now we consider the case of two different solutions $|\psi\rangle \neq |\phi\rangle$ and define $v_{1,2} := \langle\psi|W_j|\phi\rangle$. If their eigenvalues do not satisfy $\lambda_1 \lambda_2^* = 1$, then the current between these two solutions is zero $v_{1,2} = 0$. So let's assume $\lambda_1 = 1/\lambda_2^*$. Because if $|\lambda_1| > 1$ then $|\lambda_2| < 1$, a current can flow between an evanescent left going wave and an evanescent right going wave. But if we restrict ourselves to solutions with finite amplitudes in a semi-infinite lead, then either the left or right going wave amplitude must be zero. Therefore evanescent waves do neither carry a current themselves nor do they exchange current with other channels, that is they do not at all contribute to the net current.

Finally we are left with the case $\lambda_1 = 1/\lambda_2^*$, with $|\lambda_1| = |\lambda_2| = 1$. This is equivalent to $\lambda_1 = \lambda_2$, i.e. the case of degenerate eigenvalues. Therefore propagating waves to degenerate eigenvalues do exchange current. That in turn means, that the current of a superposition of two such waves does not necessarily equal the sum of the two individual currents, which is problematic as we want to express the total current as a sum of independent channels. However, the propagating and evanescent waves were obtained by diagonalising the propagator P . This transformation is unique up to rotations in every degenerate eigenvalue subspace. Because W is anti-hermitian we can diagonalise these subspaces and the resulting diagonal elements will be purely imaginary. So the net current may be written as a summation over all the individual contributions of propagating channels, only if these subspace rotations are performed.

Summarising we have shown that the transformation U diagonalising the propagator P (i.e. $U^{-1}PU$) can be chosen such that the transformation $U^\dagger W U$ of the current operator is diagonal in the subspace of propagating waves with purely imaginary diagonal elements. All the other diagonal entries are zero and the only non-zero non-diagonal elements belong to evanescent waves in opposite directions.

APPENDIX B: CALCULATION OF THE SCATTERING MATRIX

The part of the Hamiltonian containing the molecular region and its coupling to the leads can be written as

$$(H - ES)|\psi\rangle = \begin{bmatrix} h_1 & M_1 & 0 & 0 & \tau_1^\dagger \\ 0 & 0 & h_2 & M_2 & \tau_2^\dagger \\ 0 & \tau_1 & 0 & \tau_2 & M_0 \end{bmatrix} |\psi\rangle = 0. \quad (\text{B1})$$

(Using this order for the coefficients it is straight forward to extend all formulas to the general case of more than two leads.) The indices 1 and 2 indicate source and drain lead surface layers, while the index 0 is used for the molecular region. $\tau_{1,2}$ are the coupling matrices from source/drain to the molecules.

We now transform into the basis of incoming and outgoing channels, i.e. we apply

$$U = \begin{bmatrix} U^1 & 0 & 0 \\ 0 & U^2 & 0 \\ 0 & 0 & 1 \end{bmatrix}, \quad \text{with } U^i = \begin{bmatrix} U_{>}^i & U_{<}^i \\ U_{>}^i \Lambda_{>}^i & U_{<}^i \Lambda_{<}^i \end{bmatrix}$$

from the right to equation (B1):

$$(H - ES)U = \begin{bmatrix} A_{>}^1 & A_{<}^1 & 0 & 0 & \tau_1^\dagger \\ 0 & 0 & A_{>}^2 & A_{<}^2 & \tau_1^\dagger \\ B_{>}^1 & B_{<}^1 & B_{>}^2 & B_{<}^2 & M_0 \end{bmatrix}, \quad (\text{B2})$$

with

$$\begin{aligned}A_{\gtrless}^i &= h_i U_{\gtrless}^i + M_i U_{\gtrless}^i \Lambda_{\gtrless}^i, \quad \text{and} \\ B_{\gtrless}^i &= \tau_i U_{\gtrless}^i \Lambda_{\gtrless}^i.\end{aligned}$$

The first and third column act on the surface layer of the incoming channels, the second and fourth act on outgoing ones, while the fifth column, acting on the molecular region, remains unchanged.

The scattering matrix expresses the outgoing channel amplitudes in terms of the incoming ones. Therefore we split the matrix of equation (B2) into two parts, one containing the outgoing columns, the other one containing the incoming ones as well as the molecular column:

$$\begin{aligned}M_{\text{out}} &:= \begin{bmatrix} A_{<}^1 & 0 & \tau_1^\dagger \\ 0 & A_{<}^2 & \tau_2^\dagger \\ B_{<}^1 & B_{<}^2 & M_0 \end{bmatrix} \quad \text{and} \\ M_{\text{in}} &:= \begin{bmatrix} A_{>}^1 & 0 \\ 0 & A_{>}^2 \\ B_{>}^1 & B_{>}^2 \end{bmatrix}.\end{aligned}$$

The first matrix M_{out} is a square matrix and by inverting it, we obtain the scattering matrix

$$s = -M_{\text{out}}^{-1} \cdot M_{\text{in}}. \quad (\text{B3})$$

-
- ¹ S. Datta, W. Tian, S. Hong, R. Reifenberger, J. I. Henderson, and C. P. Kubiak, *Phys. Rev. Lett.* **79**, 2530 (1997).
- ² M. Magoga and C. Joachim, *Phys. Rev. B* **56**, 4722 (1997).
- ³ E. G. Emberly and G. Kirczenow, *Phys. Rev. B* **64**, 235412 (2001).
- ⁴ P. A. Derosa and J. M. Seminario, *J. Phys. Chem. B* **105**, 471 (2001).
- ⁵ P. Damle, A. W. Ghosh, and S. Datta, *Chem. Phys.* **281**, 171 (2002).
- ⁶ M. Brandbyge, J. L. Mozos, P. Ordejon, J. Taylor, and K. Stokbro, *Phys. Rev. B* **65**, 165401 (2002).
- ⁷ P. S. Krstic, X. G. Zhang, and W. H. Butler, *Phys. Rev. B* **66**, 205319 (2002).
- ⁸ A. Nitzan and M. A. Ratner, *Science* **300**, 1384 (2003).
- ⁹ C. J. F. Dupraz, U. Beierlein, and J. P. Kotthaus, *ChemPhysChem* (to be published).
- ¹⁰ P. Sautet and C. Joachim, *Chem. Phys. Lett.* **185**, 23 (1989).
- ¹¹ J. Chen, M. A. Reed, A. M. Rawlett, and J. M. Tour, *Science* **286**, 1550 (1999).
- ¹² M. A. Reed, C. Zhou, C. J. Muller, T. P. Burgin, J. M. Tour, *Science* **278**, 252 (1997).
- ¹³ J. Reichert, R. Ochs, D. Beckmann, H. B. Weber, M. Mayor, and H. v. Löhneysen, *Phys. Rev. Lett.* **88**, 176804 (2002).
- ¹⁴ J.-O. Lee, G. Lientschnig, F. Wiertz, M. Struijk, R. A. J. Janssen, R. Egberink, D. N. Reinhoudt, P. Hadley, and C. Dekker, *Nano Lett.* **3**, 113 (2003).
- ¹⁵ M. H. Hettler, W. Wenzel, M. R. Wegewijs, and H. Schoeller, *Phys. Rev. Lett.* **90** 076805 (2003).
- ¹⁶ M. J. Frisch, G. W. Trucks, H. B. Schlegel, G. E. Scuseria, M. A. Robb, J. R. Cheeseman, V. G. Zakrzewski, J. A. Montgomery, Jr., R. E. Stratmann, J. C. Burant, S. Dapprich, J. M. Millam, A. D. Daniels, K. N. Kudin, M. C. Strain, O. Farkas, J. Tomasi, V. Barone, M. Cossi, R. Cammi, B. Mennucci, C. Pomelli, C. Adamo, S. Clifford, J. Ochterski, G. A. Petersson, P. Y. Ayala, Q. Cui, K. Morokuma, D. K. Malick, A. D. Rabuck, K. Raghavachari, J. B. Foresman, J. Cioslowski, J. V. Ortiz, A. G. Baboul, B. B. Stefanov, G. Liu, A. Liashenko, P. Piskorz, I. Komaromi, R. Gomperts, R. L. Martin, D. J. Fox, T. Keith, M. A. Al-Laham, C. Y. Peng, A. Nanayakkara, C. Gonzalez, M. Challacombe, P. M. W. Gill, B. G. Johnson, W. Chen, M. W. Wong, J. L. Andres, M. Head-Gordon, E. S. Replogle and J. A. Pople, *Gaussian 98 (Revision A.7)*, Gaussian, Inc., Pittsburgh PA, 1998.
- ¹⁷ S. Datta, *Electronic Transport in Mesoscopic Systems*, Cambridge University Press, Cambridge, U. K., 1995.
- ¹⁸ D. S. Fisher and P. A. Lee, *Phys. Rev. B* **23**, 6851 (1981).
- ¹⁹ P. Sautet and C. Joachim, *Phys. Rev. B* **38**, 12238 (1988).
- ²⁰ D. Rosh, PhD Thesis, University of Cambridge (1992).
- ²¹ C. Zeng, B. Li, B. Wang, H. Wang, K. Wang, J. Yang, J. G. Hou, and Q. Zhu, *J. Chem. Phys.* **117**, 851 (2002).
- ²² Y. Yourdshahyan and A. M. Rappe, *J. Chem. Phys.* **117**, 825 (2002).
- ²³ C. W. Bauschlicher, A. Ricca, N. Mingo, J. Lawson, *Chem. Phys. Lett.* **372**, 723 (2003).